CHAPTER 5

MODELLING AND REDUCTION OF NON-CUTTING ENERGY CONSUMPTION AND CARBON EMISSIONS

In this chapter, the fixed/non-cutting energy consumption of a machine tool during milling process is analyzed and reduced without affecting machining quality. A micro analysis based methodology is developed to identify non value adding activities and Therbligs. A value stream mapping technique in conjunction with Therblig based models is used for the assessment of energy consumption, time to process and carbon emissions for a milling process. A case study is provided to illustrate the proposed methodology.

5.1 INTRODUCTION

The complex structure and large number of energy consuming components in a machine tool provide a constant challenge to the researchers to characterize and model the energy consumption during machining process. The fixed energy or non-cutting energy constitutes up to 85% of the total energy consumed by the machine tool during the machining process. Therefore, analysis of fixed energy is important to improve the energy efficiency of the machining process.

The most widely used fixed energy saving strategies include energy efficient design of machine tools and process planning at micro and macro levels. Energy efficient design includes reduction of the weight of the machine tools and selection of energy efficient components. At macro process planning stage, the energy saving strategies include (i) selection of suitable machine tools and machining processes to execute the required machining tasks and (ii) energy efficient scheduling of machining operations. At micro process planning stage, the energy saving potential of machining processes can be identified by understanding the energy consumption behavior of energy consuming components of machine tools. Some studies have been conducted with a focus on the fixed energy consumption of machine tools and measures are proposed to reduce it in both, design and operation phases (Li et al., 2011). The machine tool energy decomposition and the energy saving strategies are discussed in chapter 2.

Several studies have discussed the energy decomposition of machine tools at component level (Götze et al., 2012; Luan et al., 2018; Moradnazhad and Unver, 2017; Shen et al., 2018; Triebe et al., 2018; Wei et al., 2018). The mathematical and experimental models to estimate the energy consumed by one or more components are provided (Borgia et al., 2017; He et al., 2012; Lenz et al., 2017). However, these models do not explain the energy flow at micro level. Therblig based energy modelling methodology for a machining process was first proposed by Jia et al. (2014), where Therblig was considered as the basic energy demand unit. Therblig based analysis can provide a deep insight into the motion and energy demand of a machining process (Jia et al., 2014). The proposed energy demand modelling methodology divided the machining processes into a series of activities and Therbligs; and linked them with the machining state. Therblig power models for calculating the energy supply of CNC machine tools using machining process parameters were developed by Lv et al. (2014). Jia et al. (2016) also provided a methodology to divide a machining process into activities using Therblig activation information. Therblig based energy models were further used to model the energy consumption during transient states (Jia et al., 2017a). However, it was difficult to predict the non-value added energy from these models. Jia et al. (2017b) proposed, for the first time, a Therblig embedded value stream mapping (TVSM) method to improve the energy transparency, which clearly showed the energy waste during machining. The proposed TVSM enables the user to improve time and energy efficiencies in machining without decreasing the machining quality. The above papers (Jia et al., 2017b, 2016, 2014; Lv et al., 2014) validated the proposed models for turning processes. VSM is a widely used and proven method that enables mapping and analysis to drive potentials for improvement (Meudt et al., 2017). However, the TVSM proposed by Jia et al., (2017b) has two shortcomings: (i) it does not depict the energy of each activity on the TVSM; it only sums up the Therblig energy for the whole machining process instead of summation for each activity. This inhibits the energy flow transparency of the machining process on the value stream map and (ii) it does not reflect the energy saving in FSM for the improvements at the activity level. The basic use of any VSM is to provide a kaleidoscopic view of the value chain under analysis so that potentials for improvement are visually reflected. Depiction of time and energy on the VSM for each activity was also endorsed by Müller et al. (2014). Incorporation of the energy information visually through VSM increases its usefulness as a tool to assess the energy flow in the machining operations (Faulkner and Badurdeen, 2014).

It has been observed that the energy consumption by non-cutting operations varies with machine tools for a milling process whereas for a turning process it is almost independent of the machine tools (Lv et al., 2016). The energy consumed by non-cutting operations is complex for a milling process as compared to a turning process; and hence, detailed analysis of fixed energy consumption for a milling process is necessary (Lv et al., 2016). Therblig based value stream mapping for a milling process has not been carried out yet. The modelling of carbon emissions during machining processes has also received less attention despite its high contribution to environmental impacts. More than 99% of the carbon emissions from a machining process are caused by the electrical energy consumption (Li et al., 2011). Information about carbon emissions caused by value added and non-value added activities will help to optimize the value streams from environmental impact perspective. A model to precisely determine and monitor the carbon emissions, processing time and energy flow in a milling process is yet to be undertaken. Therefore, this chapter provides an improved micro analysis based methodology, which visually depicts the whole manufacturing processes energy flow and carbon emissions on the value stream map to assist the decision makers by getting a kaleidoscopic view of the process, activities and Therbligs with energy and carbon emissions data. The VSM is extended to energy and carbon emissions value steam mapping while maintaining its original character and its inner logic. The main contributions of the present study are:

- Therblig based value stream map was developed for milling process.
- Total energy consumed by milling process was decomposed to obtain energy consumption for each activity and each component.
- Energy consumption and carbon emissions for each activity were included on the value stream maps.
- Energy consumption and carbon emission hotspots were identified; and improvement strategies were implemented

5.2 METHODOLOGY

This section presents the methodology developed for the study. The machining process is divided into activities and activities are divided into Therbligs. In CNC machining operations, 14 types of Therbligs are used, as shown in Table 5.1.

Table 5.1 List of Therbligs used in machining process (Jia et al., 2014)

S. No.	Therblig	Representation	Symbol
1	Stand-by	SB	
2	Light	L	
3	Coolant supply	CS	
4	Spindle rotation	SR	
5	Chip convey	CC	
6	X-axis feed	XF	
7	Y-axis feed	YF	
8	Z-axis feed	ZF	
9	A-axis rotation	AR	
10	B-axis rotation	BR	
11	C-axis rotation	CR	
12	Tool selection	TS	
13	Tool change	TC	
14	Cutting	C	

These are the basic energy consuming elements for machining operations. The framework of methodology adopted for the present study is shown in Figure 5.1. It consists of three major phases: data collection, value stream mapping and result analysis.

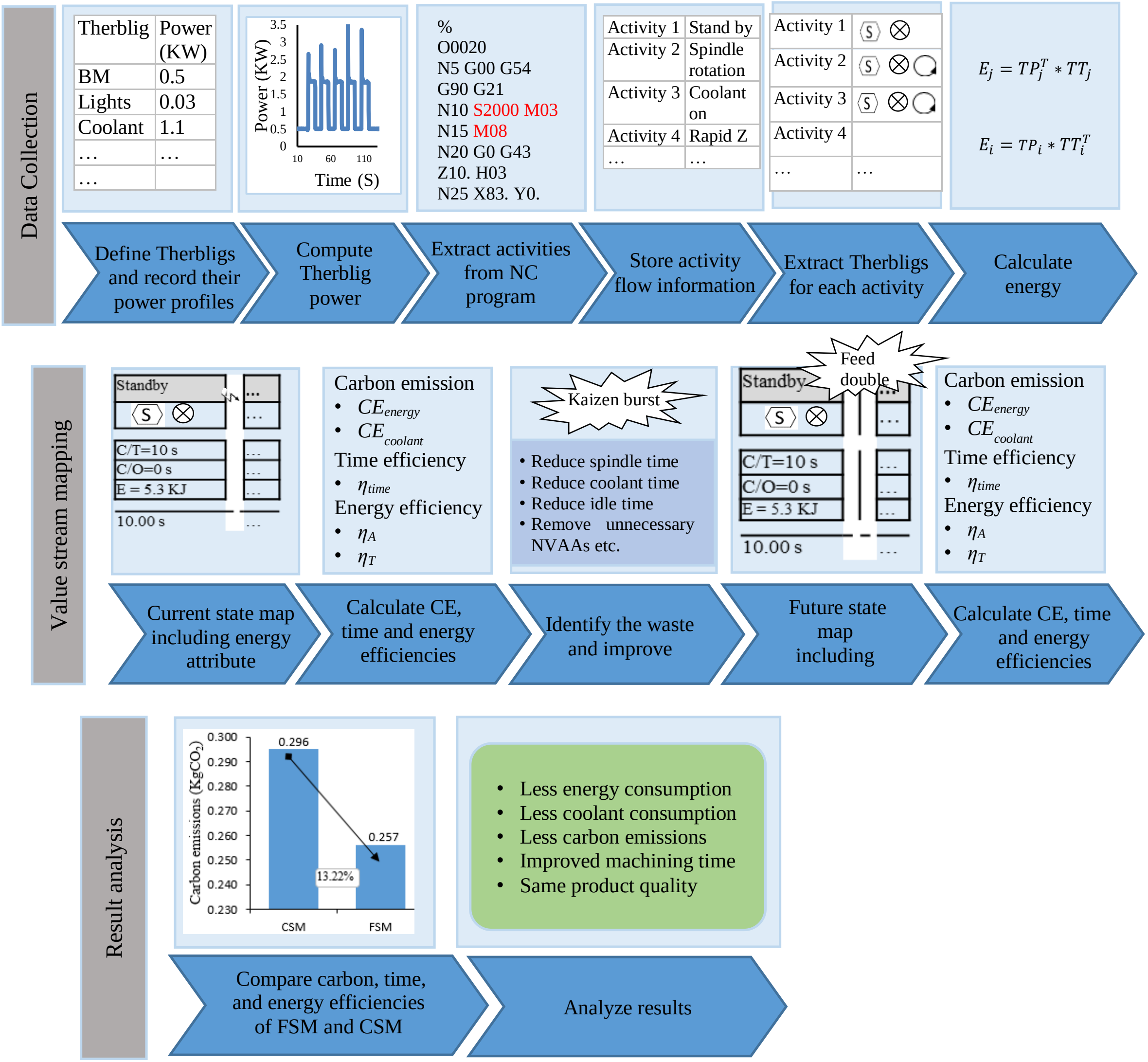

Figure 5.1 Methodology adopted for the present study

5.2.1 Define Therbligs and Calculate the Therblig Power

Micro-motion study was used to divide the machining operation into basic motion elements known as Therbligs. Therbligs were categorized into two types: constant power Therbligs and variable power Therbligs. The power required for execution of a Therblig was defined as Therblig power.

Constant power Therbligs are not directly related to material removal. Power consumed by these Therbligs is constant and does not depend on the cutting parameters and the power drawn by these Therbligs was determined through experimental studies. For example, stand-by, lights, coolant supply, tool selection, tool change, chip conveyor Therbligs are constant power Therbligs. In the present study, each component was activated for five times to record their power profiles and the mean of five power values was computed to determine the corresponding Therblig power. Variable power Therbligs are directly related to material removal. Power consumed by these Therbligs is not constant and depends on the cutting parameters. For example, spindle rotation, feed motion, cutting, etc. The power of the variable power Therbligs was computed using experimental studies and statistical analysis. The detailed methodology to determine the power for these Therbligs is provided in the literature (He et al., 2012; Lv et al., 2014).

5.2.2 Extract the Activities from the NC Program and Store the Activity Flow Information

Machining activities involve the execution of certain operations by machine tools. This information is provided to the machine tool in the form of NC programs. Therefore, all information about the machining was extracted from the NC programs. The activity flow information and the duration of each activity were stored.

5.2.3 Extract the Therbligs from Activities and Calculate Execution Time of each Therblig

One or more Therbligs can be executed in one activity. Therbligs associated with each activity were extracted and stored. The execution time of each Therblig in an activity was calculated as a product of the activity duration and the execution state of the Therblig. The execution state of the Therblig was represented as 0 for non-execution of Therbligs and 1 for execution of Therbligs. The Therblig time (TT) was represented in a matrix:

$$TT = \mathrm{T} * \mathrm{ATR} = \begin{bmatrix} t_1 * s_{11} & t_1 * s_{12} & \cdots & t_1 * s_{1m} \\ t_2 * s_{21} & t_2 * s_{22} & \cdots & t_2 * s_{2m} \\ \vdots & \vdots & \ddots & \vdots \\ t_n * s_{n1} & t_n * s_{n2} & \cdots & t_n * s_{nm} \end{bmatrix} \tag{5.1}$$

where ATR = activity Therblig relationship, n= number of extracted activities, m = number of Therbligs, $t_i(\mathrm{i} = 1, \ldots, \mathrm{n})$ = duration of i^{th} activity, and s_{ij} (i =1,…,n; j= 1,…,m) is the execution state of j^{th} Therblig in i^{th} activity. The Therblig powers (TP) were also represented in matrix form:

$$TP = \begin{bmatrix} p_{11} & p_{12} & \cdots & p_{1m} \\ p_{21} & p_{22} & \cdots & p_{2m} \\ \vdots & \vdots & \ddots & \vdots \\ p_{n1} & p_{n2} & \cdots & p_{nm} \end{bmatrix} \tag{5.2}$$

where p_{ij} is the power of j^{th} Therblig in i^{th} activity. The calculation of p_{ij} is explained in section 5.2.1.

5.2.4 Calculate Energy for each Therblig (E_j) and Activity (E_i)

Energy consumed by Therblig j (E_j) was calculated as:

$$E_j = TP_j^T * TT_j = \begin{bmatrix} p_{1j} \\ p_{2j} \\ \vdots \\ p_{nj} \end{bmatrix}^T * \begin{bmatrix} t_1 * s_{1j} \\ t_2 * s_{2j} \\ \vdots \\ t_n * s_{nj} \end{bmatrix}$$

$$= p_{1j} * \left(t_1 * s_{1j}\right) + p_{2j} * (t_2 * s_{2j}) + \cdots + p_{nj} * (t_n * s_{nj}) \tag{5.3}$$

Energy consumption for execution of each machining activity was calculated using the power consumed by the Therbligs associated with that activity and duration of the activity. Energy consumed by activity i (E_i) was calculated as:

$$E_i = TP_i * TT_i^T = [p_{i1} \quad p_{i2} \quad \cdots \quad p_{im}] * [(t_1 * s_{i1}) \quad (t_1 * s_{i2}) \quad \dots \quad (t_1 * s_{im})]^T$$

$$= p_{i1} * (t_1 * s_{i1}) + p_{i2} * (t_1 * s_{i2}) + \cdots + p_{im} * (t_1 * s_{im}) \qquad (5.4)$$

Sum of energy consumed by all the Therbligs provided the total energy consumption by the machining process.

5.2.5 Develop Current State Map (CSM) and Future State Map (FSM)

Energy flow was mapped using value stream mapping (VSM) technique adopted from industrial engineering. It is an effective tool to visualize the material, energy and information flow as the product passes through the various activities. This helps in identifying the non-value added activities to be eliminated for better efficiencies in general and in this research particularly the energy efficiency. After locating the energy wastes, measures are taken to reduce or eliminate the energy waste and future state map is obtained. From energy efficiency perspective, Therbligs are classified as value added Therbligs (VAT) and non-value added Therbligs (NVAT). Therbligs directly associated with material removal are classified as VATs and the Therbligs which are not directly related to material removal are classified as NVATs. A machining activity consisting VATs is known as value added activity (VAA) and an activity consisting only NVATs is known as non-value added activity (NVAA). Non-value added activities and Therbligs are further classified as necessary and unnecessary non-value added activities and Therbligs. Unnecessary non-value added activities (UNVAA) are those activities where all the Therbligs can be eliminated. If only a few Therbligs can be eliminated then the activity is known as necessary non-value added activity (NNVAA). Unnecessary non-value added activities (UNVAA) and Therbligs are reduced or eliminated using the value stream analysis.

5.2.6 Analyze the Machining Performance for Energy Efficiency and Carbon Performance

The proposed methodology for energy and carbon efficient machining was evaluated by calculating the four performance measures:

a) Carbon emissions

In machining processes, the carbon emissions are caused due to various factors such as energy consumption by the machine tool, production of raw material, consumption of cutting tools, production and disposal of coolant used, metal chip post-processing, etc. The carbon emissions refer to the amount of CO_2 generated during the machining process. It is measured in kg-CO_2 equivalent. In this study, only the carbon emissions caused by energy (CE_{energy}) and coolant ($CE_{coolant}$) consumption were considered as these are two major factors responsible for the carbon emissions during a machining process, in addition to the raw material. Since the cutting parameters were not varied in this study, the tool life and the amount of chip generated did not vary. Therefore, the carbon emissions caused due to cutting tool production and chip post-processing were not considered.

The carbon emissions caused by electrical energy consumption were calculated as:

$$CE_{energy} = CEF_{energy} * EC_{process} \tag{5.5}$$

where CEF_{energy} is the carbon emission factor for electricity and $EC_{process}$ is the energy consumed during the machining process. In this study, the carbon emission factor was taken from the Eco-invent dataset 3.0 for 1 kWh Indian electricity mix. The carbon emissions were measured in kgCO_2 equivalent per kWh.

The carbon emissions caused by coolant consumption were calculated as:

$$CE_{coolant} = \frac{PT}{T_{coolant}} * [CEF_{coolant} * (V_{in} + V_{ad}) + CEF_{coolant-dis} * \frac{(V_{in} + V_{ad})}{\delta} \quad (5.6)$$

where $T_{coolant}$ is the average interval of coolant change, PT is the processing time, $CEF_{coolant}$ and $CEF_{coolant-dis}$ are the carbon emission factors for production and disposal of coolant respectively, V_{in} is the volume of cutting fluid used initially, V_{ad} is the volume of additional cutting fluid used before coolant replacement, and δ is the concentration of the coolant. $CEF_{coolant}$ was computed based on the embodied energy and the carbon intensity of the cutting fluid. It was measured in $kgCO_2$/kg of the cutting fluid. Generally, two types of cutting fluids are used in machining operations, water- based and oil-based cutting fluids. In the present study, water soluble mineral oil with 5% concentration (5% mineral oil + 95% water) was used as a cutting fluid. The values of $CEF_{coolant}$ and $CEF_{coolant-dis}$ were acquired from the literature (Yi et al., 2015).

b) Time efficiency (η_{time})

Time efficiency defines how much time was utilized for actual material removal out of the total machining time and was calculated as:

$$\eta_{time} = \frac{sum\ of\ duration\ of\ VAAs}{Total\ machining\ time} \quad (5.7)$$

c) Energy efficiency

Energy efficiency of the machining process is defined at activity and Therblig levels. The energy efficiency at the activity level (η_A) is defined as the ratio of energy consumed by value added activities, i.e. cutting activities to the total energy consumption of the process. It was calculated as:

$$\eta_A = \frac{sum\ of\ energy\ consumed\ by\ VAAs}{Total\ energy\ consumed\ in\ machining\ process} \quad (5.8)$$

The cutting activities involve more than one Therbligs in each activity such as stand-by, lights, coolant supply. Feeds in x, y, z directions, and cutting Therblig. However, the cutting Therblig is the only value added Therblig (VAT). Therefore, only cutting Therblig contributes to the energy efficiency at Therblig level (η_T), which is calculated as:

$$\eta_T = \frac{sum\ of\ energy\ consumed\ by\ VATs}{Total\ energy\ consumed\ in\ machining\ process} \tag{5.9}$$

5.3 CASE STUDY

In the current study, the proposed methodology was illustrated with a milling case study. The machining experiments were conducted on a three axis CNC vertical milling center (VMC). The detailed information about the technical specifications of the machine tool is given in Chapter 3 (section 3.2). A cuboidal aluminum block of size 75×75×50 mm^3 was used as a workpiece. Six machining operations were conducted on the workpiece:

Operation 1: Face milling to remove 1 mm layer from surface using 25 mm face mill

Operation 2: Drilling a hole (Φ7mm x 30mm depth) using 7 mm drill

Operation 3: Making a slot (slot A) (23mm x 8mm x 2mm) using 6 mm end mill

Operation 4: Making a side slot (slot B) (21mm x 8mm x 2mm) using 6 mm end mill

Operation 5: Making a pocket (15mm x 15mm x 3mm) using 6 mm end mill

Operation 6: Making a slot (slot C) (30mm x 12mm x 4mm) using 10 mm end mill

The drilling operation is also included in the case study as this is a widely used process in the milling machine tools. The power profile for the machining process was recorded at the main power supply of the machine as shown in Figure 5.2. Fluke 435 series ii three-phase power quality and energy analyzer was used to record the power. The details of the workpiece and cutting conditions used for the study are provided in Figure 5.3 and Table 5.2, respectively.

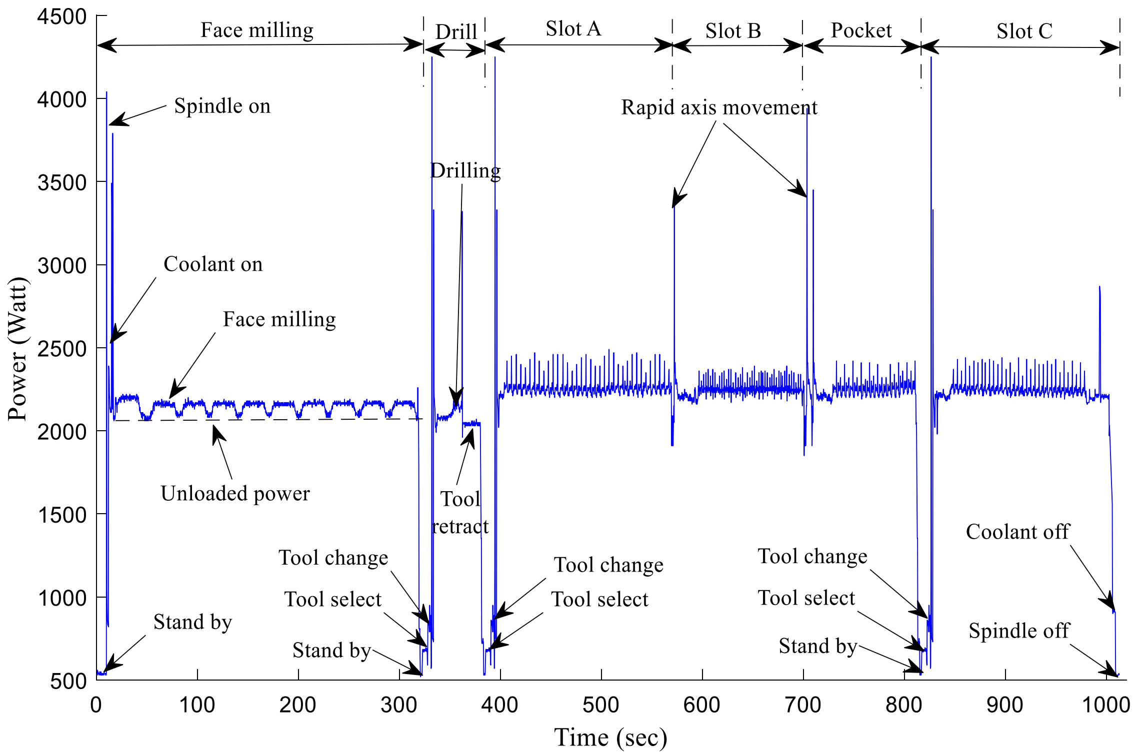

Figure 5.2 Power profile recorded for the case study

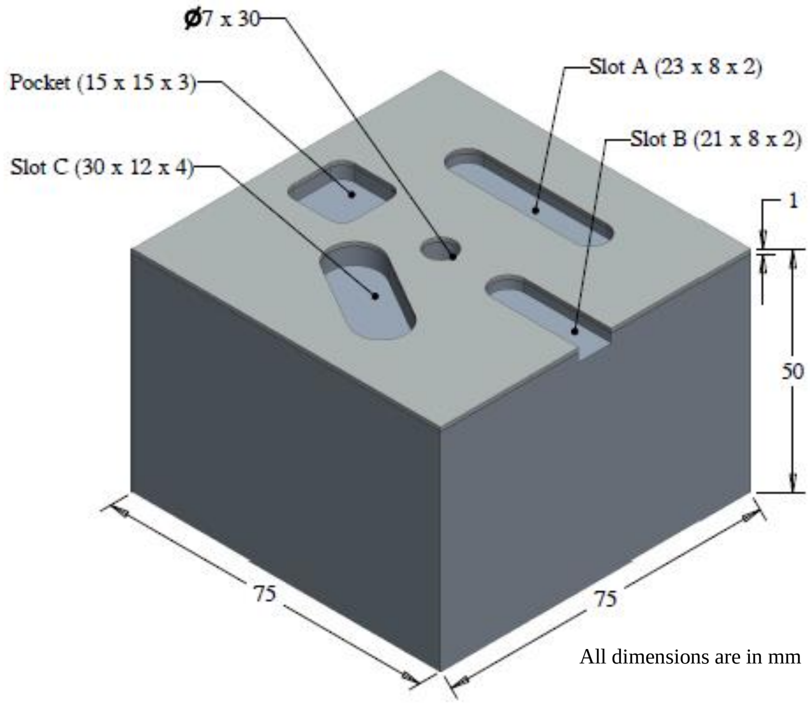

Figure 5.3 Workpiece and operations used for the case study

Table 5.2 Cutting conditions used for the case study

Operation number	Cutting speed (RPM)	Feed (mm/min)	Depth of cut (mm)	Width of cut (mm)
1	2000	200	1	7.5
2	1500	50	-	-
3	2000	100	0.5	6
4	2000	100	1	6
5	2000	100	0.5	6
6	2000	100	1	10

5.3.1 Calculate the Therblig Power

The power consumption for spindle rotation and feed axis motors depend upon the machining parameters. The mathematical models for unloaded spindle rotation and feed-axis motors have been provided in Chapter 3 (section 3.3.3 and 3.3.4). These models were used here to obtain the Therblig powers for unloaded spindle rotation and axis movements. The power consumption for auxiliary components is also given in Chapter 3 (section 3.3.5). The Therblig powers (see Table 5.3) were obtained based on the energy models provided in Chapter 3.

Table 5.3 Therblig powers for machining operation on LMW klein Kodi 40 VMC

S.No.	Therblig	Power consumption (kW)
1	Basic Module	0.5
2	Lights	0.03
3	Coolant supply	1.1
4	X-axis feed motion (200, 400)	0.04, 0.04
5	Y-axis feed motion (200, 400)	0.04, 0.04
6	Z-axis feed motion (200, 400)	0.09, 0.09
7	X-axis rapid motion	0.36
8	Y-axis rapid motion	0.36
9	Z-axis rapid motion	1.14
10	Tool selection	0.18
11	Tool change	0.25

5.3.2 Extract the Activities from the NC Program

The activities executed for the machining operations were extracted from the NC program. To perform the required six machining operations, 215 machining activities were executed. The activities and their corresponding durations are shown in Table 5.4. After extracting the activities, the Therbligs associated with each activity were identified. Table 5.4 presents the list of activities, their duration, and Therbligs.

Table 5.4 Extracted activities with time durations and corresponding Therbligs

				Corresponding Therbligs									
S.No.	**Activity**	**Distance (mm)**	**Duration(s)**	**SO**	**L**	**CFS**	**SR**	**XF**	**YF**	**ZF**	**TS**	**TC**	**C**
1	Stand by operation		10	√	√								
2	Spindle rotation (@2000RPM)		2	√	√		√						
3	Coolant on		3	√	√	√	√						
4	Rapid Z (20m/min)	174	0.52	√	√	√	√			√			
5	Rapid X-Y (24m/min)	120	0.3	√	√	√	√	√	√				
6	Rapid Y	20	0.05	√	√	√	√		√				
7	Rapid Z	5	0.015	√	√	√	√			√			
8	Feed Z (200mm/min)	6	1.8	√	√	√	√			√			
9	Cutting X	91	27.3	√	√	√	√	√					√
10	Feed Y	7.5	2.25	√	√	√	√		√				
11	Cutting X	91	27.3	√	√	√	√	√					√
12	Feed Y	7.5	2.25	√	√	√	√		√				
13	Cutting X	91	27.3	√	√	√	√	√					√
14	Feed Y	7.5	2.25	√	√	√	√		√				
15	Cutting X	91	27.3	√	√	√	√	√					√
16	Feed Y	7.5	2.25	√	√	√	√		√				
17	Cutting X	91	27.3	√	√	√	√	√					√
18	Feed Y	7.5	2.25	√	√	√	√		√				
19	Cutting X	91	27.3	√	√	√	√	√					√
20	Feed Y	7.5	2.25	√	√	√	√		√				
21	Cutting X	91	27.3	√	√	√	√	√					√
22	Feed Y	7.5	2.25	√	√	√	√		√				
23	Cutting X	91	27.3	√	√	√	√	√					√
24	Feed Y	7.5	2.25	√	√	√	√		√				
25	Cutting X	91	27.3	√	√	√	√	√					√

Table 5.4 Extracted activities with time durations and corresponding Therbligs (Contd.)

S.No.	Activity	Distance (mm)	Duration(s)	Corresponding Therbligs									
				SO	L	CFS	SR	XF	YF	ZF	TS	TC	C
26	Feed Y	7.5	2.25	√	√	√	√		√				
27	Cutting X	91	27.3	√	√	√	√	√					
28	Feed Z	11	0.036	√	√	√	√			√			
29	Coolant stop		1.5	√	√		√						
30	Rapid Z	174	0.52	√	√		√			√			
31	Rapid XY	72.5	0.18	√	√		√	√	√				
32	Rapid X	47.5	0.12	√	√		√	√					
33	Spindle stop		1.5	√	√								
34	Tool select		4	√	√						√		
35	Tool change		2.5	√	√							√	
36	Spindle start (@1500 RPM)		1.5	√	√		√						
37	Coolant on		2	√	√	√	√						
38	Rapid Z	174	0.52	√	√	√	√			√			
39	Rapid XY	102.5	0.25	√	√	√	√	√	√				
40	Rapid X	63	0.16	√	√	√	√	√					
41	Cutting Z (50mm/min)	30	22	√	√	√	√			√			√
42	Feed Z (retract)	30	18	√	√	√	√			√			
43	Rapid Z	10	0.03	√	√	√	√			√			
44	Coolant stop		1.5	√	√		√						
45	Rapid Z	174	0.52	√	√		√			√			
46	Rapid XY	102.5	0.25	√	√		√	√	√				
47	Rapid X	63	0.16	√	√		√	√					
48	Spindle stop		1.5	√	√								
49	Tool select		4	√	√						√		
50	Tool change		2.5	√	√							√	
51	Spindle start (@2000 RPM)		1.5	√	√		√						
52	Coolant on		2	√	√	√	√						
53	Rapid Z	174	0.48	√	√	√	√			√			
54	Rapid X-Y	81	0.2	√	√	√	√	√	√				
55	Rapid X	84.5	0.21	√	√	√	√	√					
56	Feed Z (50 mm/min)	11	13.2	√	√	√	√			√			
57	Cutting Z (50 mm/min)	0.5	0.6	√	√	√	√			√			√
58	Cutting Y (100 mm/min)	1	0.6	√	√	√	√		√				√
59	Cutting X (100 mm/min)	15	9	√	√	√	√	√					√
60	Cutting X-Y (70.71 mm/min)	2	1.69	√	√	√	√	√	√				√
61	Cutting X (100 mm/min)	30	18	√	√	√	√	√					√
62	Cutting X-Y (70.71 mm/min)	2	1.69	√	√	√	√	√	√				√

Table 5.4 Extracted activities with time durations and corresponding Therbligs (Contd.)

S.No.	Activity	Distance (mm)	Duration(s)	Corresponding Therbligs									
				SO	L	CFS	SR	XF	YF	ZF	TS	TC	C
63	Cutting X (100 mm/min)	15	9	√	√	√	√	√					√
64	Feed Y (100 mm/min)	1	0.6	√	√	√	√		√				
65	Cutting Z (50 mm/min)	0.5	0.6	√	√	√	√			√			√
66	Cutting Y (100 mm/min)	1	0.6	√	√	√	√		√				√
67	Cutting X (100 mm/min)	15	9	√	√	√	√	√					√
68	Cutting X-Y (70.71 mm/min)	2	1.69	√	√	√	√	√	√				√
69	Cutting X (100 mm/min)	30	18	√	√	√	√	√					√
70	Cutting X-Y (70.71 mm/min)	2	1.69	√	√	√	√	√	√				√
71	Cutting X (100 mm/min)	15	9	√	√	√	√	√					√
72	Feed Y (100 mm/min)	1	0.6	√	√	√	√		√				
73	Cutting Z (50 mm/min)	0.5	0.6	√	√	√	√			√			√
74	Cutting Y (100 mm/min)	1	0.6	√	√	√	√		√				√
75	Cutting X (100 mm/min)	15	9	√	√	√	√	√					√
76	Cutting X-Y (70.71 mm/min)	2	1.69	√	√	√	√	√	√				√
77	Cutting X (100 mm/min)	30	18	√	√	√	√	√					√
78	Cutting X-Y (70.71 mm/min)	2	1.69	√	√	√	√	√	√				√
79	Cutting X (100 mm/min)	15	9	√	√	√	√	√					√
80	Feed Y (100 mm/min)	1	0.6	√	√	√	√		√				
81	Cutting Z (50 mm/min)	0.5	0.6	√	√	√	√			√			√
82	Cutting Y (100 mm/min)	1	0.6	√	√	√	√		√				√
83	Cutting X (100 mm/min)	15	9	√	√	√	√	√					√
84	Cutting X-Y (70.71 mm/min)	2	1.69	√	√	√	√	√	√				√
85	Cutting X (100 mm/min)	30	18	√	√	√	√	√					√
86	Cutting X-Y (70.71 mm/min)	2	1.69	√	√	√	√	√	√				√
87	Cutting X (100 mm/min)	15	9	√	√	√	√	√					√
88	Feed Y (100 mm/min)	1	0.6	√	√	√	√		√				
89	Feed Z (100 mm/min)	3	1.8	√	√	√	√			√			
90	Rapid Z	10	0.03	√	√	√	√			√			
91	Rapid X-Y	21.5	0.05	√	√	√	√	√	√				
92	Rapid X	21	0.05	√	√	√	√	√					
93	Feed Z (50 mm/min)	11	13.2	√	√	√	√			√			
94	Feed Z (50mm/min)	1	1.2	√	√	√	√			√			
95	Feed Y (100mm/min)	1	0.6	√	√	√	√		√				
96	Cutting X (100mm/min)	26	15.6	√	√	√	√	√					√
97	Cutting X-Y (70.71 mm/min)	2	1.69	√	√	√	√	√	√				√
98	Cutting X (100mm/min)	26	15.6	√	√	√	√	√					√
99	Feed Y (100mm/min)	1	0.6	√	√	√	√		√				

Table 5.4 Extracted activities with time durations and corresponding Therbligs (Contd.)

S.No.	Activity	Distance (mm)	Duration(s)	Corresponding Therbligs									
				SO	L	CFS	SR	XF	YF	ZF	TS	TC	C
100	Feed Z (50mm/min)	1	1.2	√	√	√	√			√			
101	Feed Y (100mm/min)	1	0.6	√	√	√	√		√				
102	Cutting X (100mm/min)	26	15.6	√	√	√	√	√					√
103	Cutting X-Y (70.71 mm/min)	2	1.69	√	√	√	√	√	√				√
104	Cutting X (100mm/min)	26	15.6	√	√	√	√	√					√
105	Feed Y (100mm/min)	1	0.6	√	√	√	√		√				
106	Feed Z (50mm/min)	1	1.2	√	√	√	√			√			
107	Feed Y (100mm/min)	1	0.6	√	√	√	√		√				
108	Cutting X (100mm/min)	26	15.6	√	√	√	√	√					√
109	Cutting X-Y (70.71 mm/min)	2	1.69	√	√	√	√	√	√				√
110	Cutting X (100mm/min)	26	15.6	√	√	√	√	√					√
111	Feed Y (100mm/min)	1	0.6	√	√	√	√		√				
112	Feed Z (100mm/min)	4	2.4	√	√	√	√			√			
113	Rapid Z	10	0.03	√	√	√	√			√			
114	Rapid X	67.5	0.17	√	√	√	√	√					
115	Feed Z (50mm/min)	11	13.2	√	√	√	√			√			
116	Cutting Z (50 mm/min)	0.5	0.6	√	√	√	√			√			√
117	Cutting X, Cutter dia compensation (100 mm/min)	4.5	2.7	√	√	√	√	√					√
118	Cutting Y (100mm/min)	4.5	2.7	√	√	√	√		√				√
119	Cutting X (100mm/min)	9	5.4	√	√	√	√	√					√
120	Cutting Y (100mm/min)	9	5.4	√	√	√	√		√				√
121	Cutting X (100mm/min)	9	5.4	√	√	√	√	√					√
122	Cutting Y (100mm/min)	4.5	2.7	√	√	√	√		√				√
123	Cutting X (100mm/min)	4.5	2.7	√	√	√	√	√					√
124	Cutting Z (50 mm/min)	0.5	0.6	√	√	√	√			√			√
125	Cutting X, Cutter dia compensation (100 mm/min)	4.5	2.7	√	√	√	√	√					√
126	Cutting Y (100mm/min)	4.5	2.7	√	√	√	√		√				√
127	Cutting X (100mm/min)	9	5.4	√	√	√	√	√					√
128	Cutting Y (100mm/min)	9	5.4	√	√	√	√		√				√
129	Cutting X (100mm/min)	9	5.4	√	√	√	√	√					√
130	Cutting Y (100mm/min)	4.5	2.7	√	√	√	√		√				√
131	Cutting X (100mm/min)	4.5	2.7	√	√	√	√	√					√
132	Cutting Z (50 mm/min)	0.5	0.6	√	√	√	√			√			√
133	Cutting X, Cutter dia compensation (100 mm/min)	4.5	2.7	√	√	√	√	√					√
134	Cutting Y (100mm/min)	4.5	2.7	√	√	√	√		√				√

Table 5.4 Extracted activities with time durations and corresponding Therbligs (Contd.)

S.No.	Activity	Distance (mm)	Duration(s)	Corresponding Therbligs									
				SO	L	CFS	SR	XF	YF	ZF	TS	TC	C
135	Cutting X (100mm/min)	9	5.4	√	√	√	√	√					√
136	Cutting Y (100mm/min)	9	5.4	√	√	√	√		√				√
137	Cutting X (100mm/min)	9	5.4	√	√	√	√	√					√
138	Cutting Y (100mm/min)	4.5	2.7	√	√	√	√		√				√
139	Cutting X (100mm/min)	4.5	2.7	√	√	√	√	√					√
140	Cutting Z (50 mm/min)	0.5	0.6	√	√	√	√			√			√
141	Cutting X, Cutter dia compensation (100 mm/min)	4.5	2.7	√	√	√	√	√					√
142	Cutting Y (100mm/min)	4.5	2.7	√	√	√	√		√				√
143	Cutting X (100mm/min)	9	5.4	√	√	√	√	√					√
144	Cutting Y (100mm/min)	9	5.4	√	√	√	√		√				√
145	Cutting X (100mm/min)	9	5.4	√	√	√	√	√					√
146	Cutting Y (100mm/min)	4.5	2.7	√	√	√	√		√				√
147	Cutting X (100mm/min)	4.5	2.7	√	√	√	√	√					√
148	Cutting Z (50 mm/min)	0.5	0.6	√	√	√	√			√			√
149	Cutting X, Cutter dia compensation (100 mm/min)	4.5	2.7	√	√	√	√	√					√
150	Cutting Y (100mm/min)	4.5	2.7	√	√	√	√		√				√
151	Cutting X (100mm/min)	9	5.4	√	√	√	√	√					√
152	Cutting Y (100mm/min)	9	5.4	√	√	√	√		√				√
153	Cutting X (100mm/min)	9	5.4	√	√	√	√	√					√
154	Cutting Y (100mm/min)	4.5	2.7	√	√	√	√		√				√
155	Cutting X (100mm/min)	4.5	2.7	√	√	√	√	√					√
156	Cutting Z (50 mm/min)	0.5	0.6	√	√	√	√			√			√
157	Cutting X, Cutter dia compensation (100 mm/min)	4.5	2.7	√	√	√	√	√					√
158	Cutting Y (100mm/min)	4.5	2.7	√	√	√	√		√				√
159	Cutting X (100mm/min)	9	5.4	√	√	√	√	√					√
160	Cutting Y (100mm/min)	9	5.4	√	√	√	√		√				√
161	Cutting X (100mm/min)	9	5.4	√	√	√	√	√					√
162	Cutting Y (100mm/min)	4.5	2.7	√	√	√	√		√				√
163	Cutting X (100mm/min)	4.5	2.7	√	√	√	√	√					√
164	Feed Z (100 mm/min)	4	1.8	√	√	√	√			√			
165	Rapid Z	10	0.03	√	√	√	√			√			
166	Coolant OFF	0	1.5	√	√		√						
167	Rapid Z	174	0.52	√	√		√			√			
168	Rapid XY	102.5	0.16	√	√		√	√	√				
169	Rapid X	87	0.22	√	√		√	√					

Table 5.4 Extracted activities with time durations and corresponding Therbligs (Contd.)

S.No.	Activity	Distance (mm)	Duration(s)	Corresponding Therbligs									
				SO	L	CFS	SR	XF	YF	ZF	TS	TC	C
170	Spindle stop			√	√								
171	Tool select		4	√	√						√		
172	Tool Change		2.5	√	√							√	
173	Spindle start (@2000 RPM)		1.5	√	√		√						
174	Coolant on		2	√	√	√	√						
175	Rapid X-Y	120.1 9	0.3	√	√	√	√	√	√				
176	Rapid X	45.31	0.11	√	√	√	√	√					
177	Rapid Z	174	0.52	√	√	√	√			√			
178	Feed Z (50mm/min)	11	13.2	√	√	√	√			√			
179	Cutting Z (50 mm/min)	1	1.2	√	√	√	√			√			√
180	Cutting X = 50mm/min Cutting Y = 86.60mm/min	1	0.6	√	√	√	√	√	√				√
181	Cutting X = 86.60 mm/min Cutting Y = 50 mm/min	9	5.4	√	√	√	√	√	√				√
182	Cutting X-Y (70.71 mm/min)	2	1.69	√	√	√	√	√	√				√
183	Cutting X = 86.60 mm/min Cutting Y = 50 mm/min	18	10.8	√	√	√	√	√	√				√
184	Cutting X-Y (70.71 mm/min)	2	1.69	√	√	√	√	√	√				√
185	Cutting X = 86.60 mm/min Cutting Y = 50 mm/min	9	5.4	√	√	√	√	√	√				√
186	Feed X = 50mm/min Feed Y = 86.60mm/min	1	0.6	√	√	√	√	√	√				
187	Cutting Z (50 mm/min)	1	1.2	√	√	√	√			√			√
188	Cutting X = 50mm/min Cutting Y = 86.60mm/min	1	0.6	√	√	√	√	√	√				√
189	Cutting X = 86.60 mm/min Cutting Y = 50 mm/min	9	5.4	√	√	√	√	√	√				√
190	Cutting X-Y (70.71 mm/min)	2	1.69	√	√	√	√	√	√				√
191	Cutting X = 86.60 mm/min Cutting Y = 50 mm/min	18	10.8	√	√	√	√	√	√				√
192	Cutting X-Y (70.71 mm/min)	2	1.69	√	√	√	√	√	√				√
193	Cutting X = 86.60 mm/min Cutting Y = 50 mm/min	9	5.4	√	√	√	√	√	√				√
194	Feed X = 50mm/min Feed Y = 86.60mm/min	1	0.6	√	√	√	√	√	√				
195	Cutting Z (50 mm/min)	1	1.2	√	√	√	√			√			√
196	Cutting X = 50mm/min Cutting Y = 86.60mm/min	1	0.6	√	√	√	√	√	√				√
197	Cutting X = 86.60 mm/min Cutting Y = 50 mm/min	9	5.4	√	√	√	√	√	√				√
198	Cutting X-Y (70.71 mm/min)	2	1.69	√	√	√	√	√	√				√

Table 5.4 Extracted activities with time durations and corresponding Therbligs (Contd.)

				Corresponding Therbligs									
S.No.	**Activity**	**Distance (mm)**	**Duration(s)**	**SO**	**L**	**CFS**	**SR**	**XF**	**YF**	**ZF**	**TS**	**TC**	**C**
199	Cutting X = 86.60 mm/min Cutting Y = 50 mm/min	18	10.8	√	√	√	√	√	√				√
200	Cutting X-Y (70.71 mm/min)	2	1.69	√	√	√	√	√	√				√
201	Cutting X = 86.60 mm/min Cutting Y = 50 mm/min	9	5.4	√	√	√	√	√	√				√
202	Feed X = 50mm/min Feed Y = 86.60mm/min	1	0.6	√	√	√	√	√	√				
203	Cutting Z (50 mm/min)	1	1.2	√	√	√	√			√			√
204	Cutting X = 50mm/min Cutting Y = 86.60mm/min	1	0.6	√	√	√	√	√	√				√
205	Cutting X = 86.60 mm/min Cutting Y = 50 mm/min	9	5.4	√	√	√	√	√	√				√
206	Cutting X-Y (70.71 mm/min)	2	1.69	√	√	√	√	√	√				√
207	Cutting X = 86.60 mm/min Cutting Y = 50 mm/min	18	10.8	√	√	√	√	√	√				√
208	Cutting X-Y (70.71 mm/min)	2	1.69	√	√	√	√	√	√				√
209	Cutting X = 86.60 mm/min Cutting Y = 50 mm/min	9	5.4	√	√	√	√	√	√				√
210	Feed X = 50mm/min Feed Y = 86.60mm/min	1	0.6	√	√	√	√	√	√				
211	Feed Z (100 mm/min)	5	3	√	√	√	√			√			
212	Rapid Z	5	0.001	√	√	√	√			√			
213	Rapid Z	179	0.53	√	√	√	√			√			
214	Coolant OFF	0	1.5	√	√		√						
215	Spindle OFF	0	1.5	√	√								

5.3.3 Calculate the Energy Demand for the Machining Process

The energy consumption for the execution of each activity and Therblig during operation 1 – 6 were calculated. Since the number of activities was large, therefore, the energy activities were divided into six parts for each of the six machining operations (face milling, drilling, slot A, slot B, pocket, and slot C) for ease of matrix representation. The activity Therblig relationship (ATR) for face milling operation (from activity 1 to activity 33) is presented below:

ATR =

1	1	1	0	0	0	0	0	0	0	0
2	1	1	0	1	0	0	0	0	0	0
3	1	1	1	1	0	0	0	0	0	0
4	1	1	1	1	0	0	1	0	0	0
5	1	1	1	1	1	1	0	0	0	0
6	1	1	1	1	0	1	0	0	0	0
7	1	1	1	1	0	0	1	0	0	0
8	1	1	1	1	0	0	1	0	0	0
9	1	1	1	1	1	0	0	0	0	1
10	1	1	1	1	0	1	0	0	0	0
11	1	1	1	1	1	0	0	0	0	1
12	1	1	1	1	0	1	0	0	0	0
13	1	1	1	1	1	0	0	0	0	1
14	1	1	1	1	0	1	0	0	0	0
15	1	1	1	1	1	0	0	0	0	1
16	1	1	1	1	0	1	0	0	0	0
17	1	1	1	1	1	0	0	0	0	1
18	1	1	1	1	0	1	0	0	0	0
19	1	1	1	1	1	0	0	0	0	1
20	1	1	1	1	0	1	0	0	0	0
21	1	1	1	1	1	0	0	0	0	1
22	1	1	1	1	0	1	0	0	0	0
23	1	1	1	1	1	0	0	0	0	1
24	1	1	1	1	0	1	0	0	0	0
25	1	1	1	1	1	0	0	0	0	1
26	1	1	1	1	0	1	0	0	0	0
27	1	1	1	1	1	0	0	0	0	1
28	1	1	1	1	0	0	1	0	0	0
29	1	1	0	1	0	0	0	0	0	0
30	1	1	0	1	0	0	1	0	0	0
31	1	1	0	1	1	1	0	0	0	0
32	1	1	0	1	1	0	0	0	0	0
33	1	1	0	0	0	0	0	0	0	0

The execution time for each activity is given in Table 5.4. The execution time of various Therbligs in each activity was calculated by multiplying the activity time matrix (T) and ATR matrix (TT= T*ATR). Therblig power matrix (TP) based on the Therblig power (Table 5.3) is:

TP =

1	0.5	0.03	0	0	0	0	0	0	0	0
2	0.5	0.03	0	0.33	0	0	0	0	0	0
3	0.5	0.03	1.1	0.33	0	0	0	0	0	0
4	0.5	0.03	1.1	0.33	0	0	1.14	0	0	0
5	0.5	0.03	1.1	0.33	0.36	0.36	0	0	0	0
6	0.5	0.03	1.1	0.33	0	0.36	0	0	0	0
7	0.5	0.03	1.1	0.33	0	0	1.14	0	0	0
8	0.5	0.03	1.1	0.33	0	0	0.09	0	0	0
9	0.5	0.03	1.1	0.33	0.04	0	0	0	0	0.15
10	0.5	0.03	1.1	0.33	0	0.04	0	0	0	0
11	0.5	0.03	1.1	0.33	0.04	0	0	0	0	0.15
12	0.5	0.03	1.1	0.33	0	0.04	0	0	0	0
13	0.5	0.03	1.1	0.33	0.04	0	0	0	0	0.15
14	0.5	0.03	1.1	0.33	0	0.04	0	0	0	0
15	0.5	0.03	1.1	0.33	0.04	0	0	0	0	0.15
16	0.5	0.03	1.1	0.33	0	0.04	0	0	0	0
17	0.5	0.03	1.1	0.33	0.04	0	0	0	0	0.15
18	0.5	0.03	1.1	0.33	0	0.04	0	0	0	0
19	0.5	0.03	1.1	0.33	0.04	0	0	0	0	0.15
20	0.5	0.03	1.1	0.33	0	0.04	0	0	0	0
21	0.5	0.03	1.1	0.33	0.04	0	0	0	0	0.15
22	0.5	0.03	1.1	0.33	0	0.04	0	0	0	0
23	0.5	0.03	1.1	0.33	0.04	0	0	0	0	0.15
24	0.5	0.03	1.1	0.33	0	0.04	0	0	0	0
25	0.5	0.03	1.1	0.33	0.04	0	0	0	0	0.15
26	0.5	0.03	1.1	0.33	0	0.04	0	0	0	0
27	0.5	0.03	1.1	0.33	0.04	0	0	0	0	0.15
28	0.5	0.03	1.1	0.33	0	0	0.09	0	0	0
29	0.5	0.03	0	0.33	0	0	0	0	0	0
30	0.5	0.03	0	0.33	0	0	1.14	0	0	0
31	0.5	0.03	0	0.33	0.36	0.36	0	0	0	0
32	0.5	0.03	0	0.33	0.36	0	0	0	0	0
33	0.5	0.03	0	0	0	0	0	0	0	0

Similarly, ATR and TP were obtained for operations 2-6. The ATR and TP for the six operations are provided in appendix A. The energy consumed by each Therblig was calculated using equation 3 and tabulated in Table 5.5. As shown in Table 5.5, the energy calculated for operations 1-6 are 650.25 kJ, 98.89 kJ, 374.81 kJ, 248.48 kJ, 369.21 kJ, and 292.77 kJ, respectively. The actual energy consumed by these operations as recorded by the energy meter were 674.983 kJ, 110.141 kJ, 385.163 kJ, 258.075 kJ, 387.269 kJ, and

299.44 kJ, respectively. The difference in the energy value is because of the transition state energy. In this study, the energy consumed during transition of one activity to other was not calculated. However, the calculated and recorded energy values are in close proximity and hence, the proposed methodology can be accepted for energy mapping.

Table 5.5 Energy consumed by various Therbligs for operations 1-6 in CSM

S No	Therblig	Energy (kJ)						
		(face mill)	(drilling)	(slot A)	(slot B)	(pocket)	(slot C)	(Total)
1	Basic Module	157.40	27.45	94.41	60.50	90.70	73.01	503.45
2	Lights	9.44	1.65	5.66	3.63	5.44	4.38	30.21
3	Coolant supply	328.87	47.26	198.89	133.10	199.54	144.11	1051.77
4	Spindle rotation	100.09	11.72	60.16	39.93	59.86	45.05	316.81
5	X-axis movement	11.14	0.30	6.45	3.98	3.95	4.51	30.32
6	Y-axis movement	1.00	0.18	0.80	0.36	2.59	4.39	9.33
7	Z-axis movement	1.37	4.82	1.95	1.05	1.76	3.88	14.83
8	Tool selection	0.00	0.72	0.72	0.00	0.00	0.72	2.16
9	Tool change	0.00	0.63	0.63	0.00	0.00	0.63	1.88
10	Cutting	40.95	4.18	5.13	5.92	5.36	12.10	73.65
	Sum	650.25	98.89	374.81	248.48	369.21	292.77	2034.40

5.3.4 Value Stream Mapping and Result Analysis

Further, the current state map of the machining process was drawn (Figure 5.4). The energy consumed by each activity was calculated using equation 4 and included in the CSM. It was found that out of 215 machining activities in CSM; only 124 were value added activities (VAA); and in each VAA there was only one value added Therblig (cutting Therblig). The duration of 124 VAAs was 828.71 seconds and the total machining duration was 1005.4 seconds.

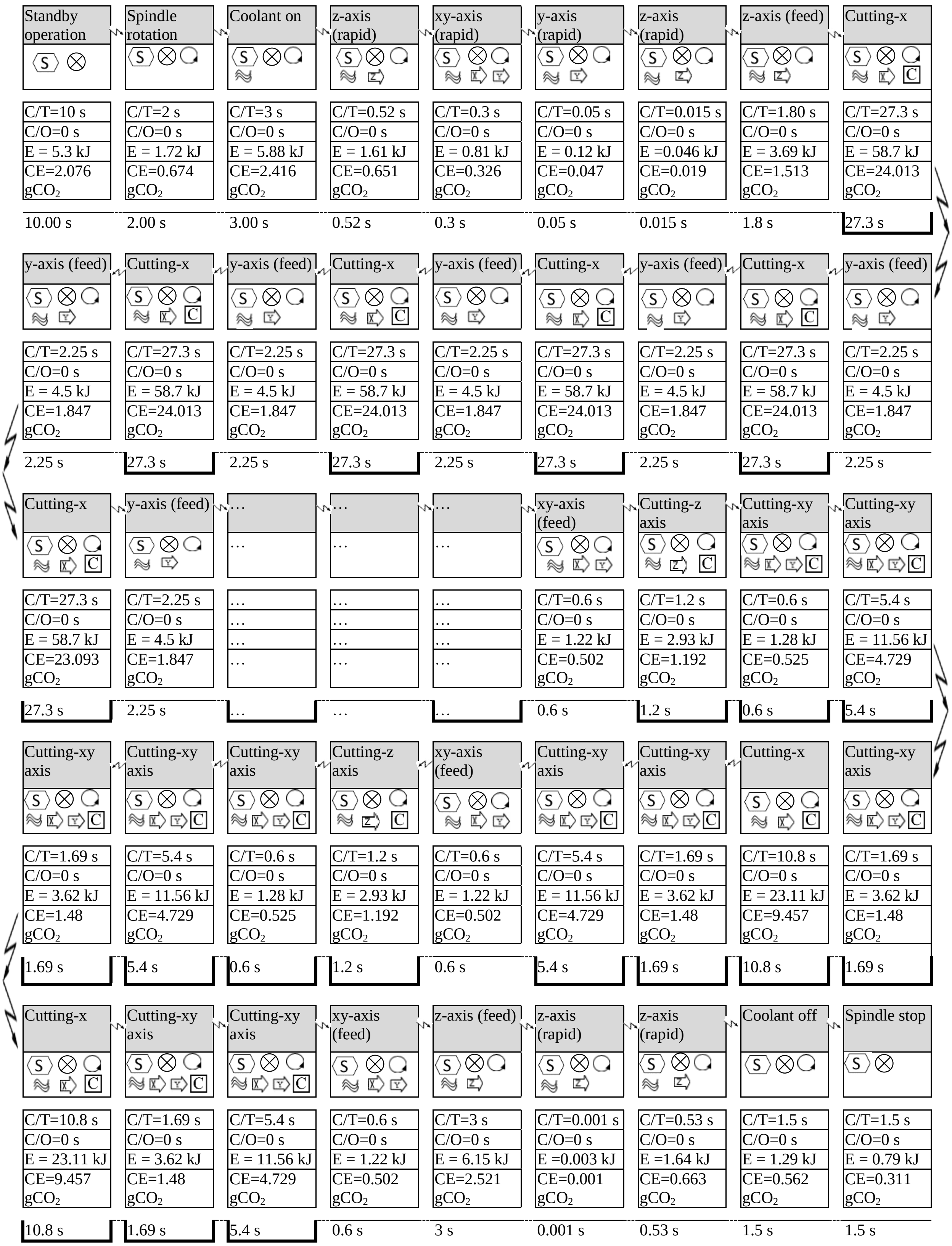

Figure 5.4 Current state mapping of the activities involved in the machining case study

The time efficiency (η_{time}), energy efficiency at the activity level (η_A) and energy efficiency at Therblig level (η_T) were calculated as shown:

$$\eta_{time} = \frac{828.71}{1005.4} = 82.43\%$$

$$\eta_A = \frac{1735.79}{2034.40} = 85.32\%$$

$$\eta_T = \frac{73.65}{2034.40} = 3.62\%$$

The parameters used for calculation of carbon emissions are provided in Chapter 4. The carbon emissions (CE) caused by energy and coolant consumption were calculated as follows:

$$CE_{energy} = \frac{2034.40 * 1.41 * 1000}{3600} = 796.81\ gCO_2$$

$$CE_{coolant} = \frac{962.15 * 1000}{3 * 30 * 8 * 3600} * [500 * (18 * 10^{-3}) + 200 * \frac{(18 * 10^{-3})}{5} = 3.61\ gCO_2$$

$$CE_{total} = 800.42\ gCO_2$$

It is evident that the time efficiency of the milling process was 82.43%, energy efficiency at activity level was 85.32%, and energy efficiency at Therblig level was 3.62%. It reveals the potential for energy and time saving in the machining process. Value stream mapping helps to thoroughly analyze energy flow and identify the energy waste. Further, the machining performance can be improved by either eliminating the NVAAs/NVATs or reducing the time or energy consumption by NVAAs/NVATs. It can be seen in Figure 5.4 that the spindle rotation and coolant supply were executed in second and third activities, respectively. However, the first material removal took place in the ninth activity and spindle rotation and coolant supply were not needed before this. Hence, both these activities could be shifted and placed before the ninth activity. This way, the spindle rotation and coolant supply Therbligs were removed from activities 4-8. This reduced the execution time and energy consumed by spindle rotation and coolant supply.

Further, in activity 8, feed motion was provided to z-axis but no cutting took place in this activity. The feed rate could be increased for this activity to reduce the execution time. Similarly, the feed rate was increased for the non-cutting movements (for example, activities 10, 12, 14, 16, 18, etc.). The non-necessary activities were also identified and removed. For example, activity 27 was redundant and therefore, could be removed. Similarly, the activities for other operations were analyzed and the improvement measures were taken. The energy and time wastes were eliminated or reduced and future state map was drawn, as shown in Figure 5.5.

The energy consumption and carbon emissions for the execution of each Therblig in future state map were calculated, as done for the current state map, and provided in Table 5.6. The energy consumption and carbon emissions caused due to each activity were also calculated and included in future state map. The time efficiency (η_{time}), energy efficiency at the activity level (η_A) and energy efficiency at Therblig level (η_T) calculated for future state map were 87.42%, 87.41%, and 3.85%, respectively. The carbon emissions caused by the energy and coolant consumption for future state map were calculated as 749.34 gCO_2 and 3.38 gCO_2, respectively. It is evident here that the energy consumption, carbon emissions and processing time have been reduced in future state map as compared to the current state map. The energy consumption by each component in future state is compared with energy consumption in the current state in the next section.

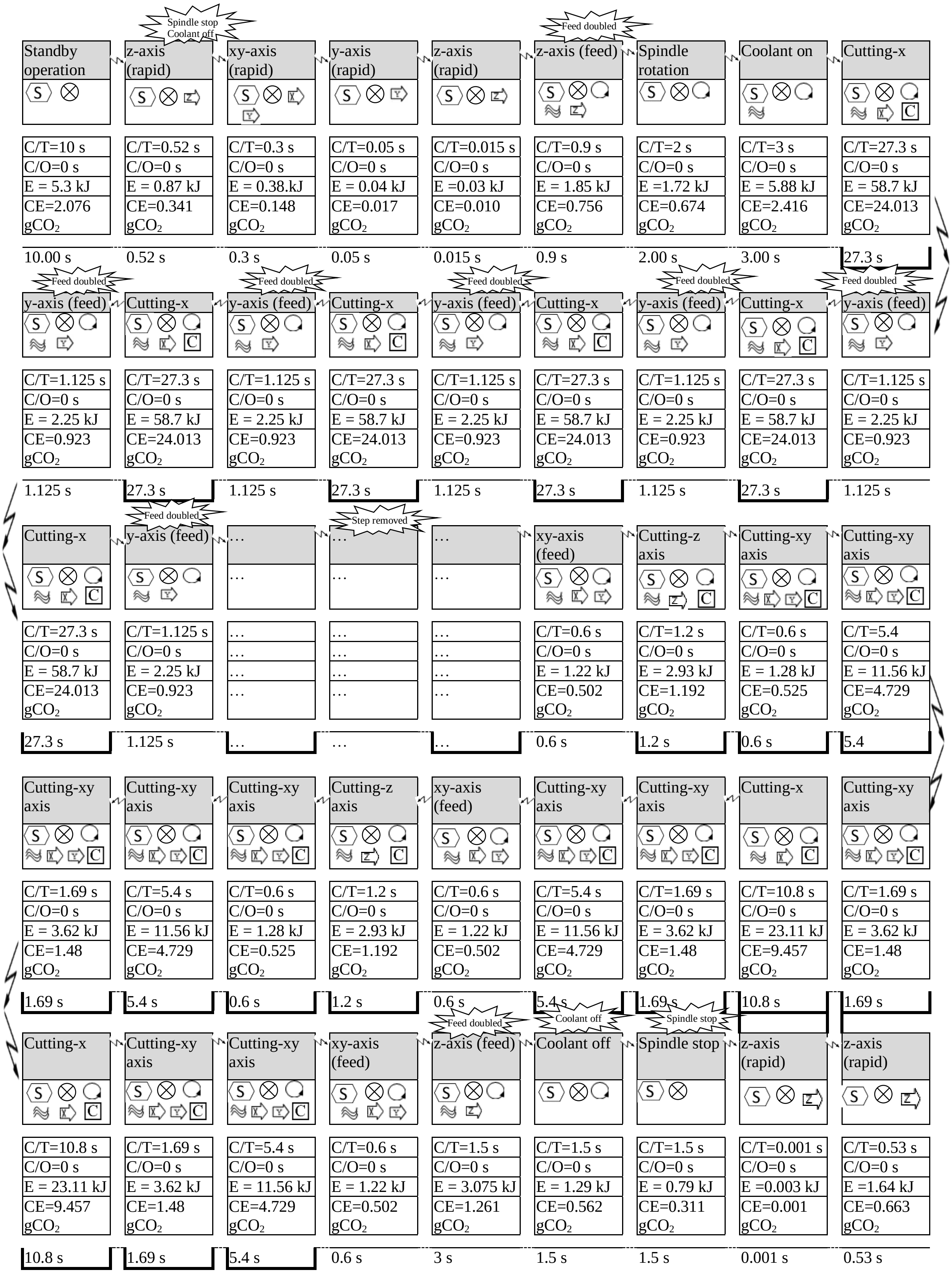

Figure 5.5 Future state mapping of the activities involved in the machining case study

Table 5.6 Energy consumed by various Therbligs for operations 1-6 in FSM

S No	Therblig	Energy (kJ)						
		(face mill)	(drilling)	(slot A)	(slot B)	(pocket)	(slot C)	(Total)
1	Basic Module	151.72	22.59	90.35	54.95	86.80	68.09	474.50
2	Lights	9.10	1.36	5.42	3.30	5.21	4.09	28.47
3	Coolant supply	315.75	36.33	189.33	120.89	190.96	132.61	985.87
4	Spindle rotation	95.88	9.14	57.29	36.27	57.29	41.27	297.13
5	X-axis movement	11.03	0.04	6.30	3.98	3.95	4.21	29.51
6	Y-axis movement	0.53	0.03	0.70	0.29	2.59	4.20	8.35
7	Z-axis movement	1.29	4.01	1.40	0.87	1.06	3.07	11.70
8	Tool selection	0.00	0.72	0.72	0.00	0.00	0.72	2.16
9	Tool change	0.00	0.63	0.63	0.00	0.00	0.63	1.88
10	Cutting	40.95	4.18	5.13	5.92	5.36	12.10	73.65
	Sum	626.25	79.02	357.28	226.47	353.22	270.98	1913.22

5.4 DISCUSSION

It can be seen here that the energy consumed by Therbligs of stand-by, lights, coolant supply, spindle rotation, and feed-x was reduced in the FSM as compared to the CSM. Figure 5.6 shows the comparison of energy consumption for these Therbligs and total machining energy in the FSM and the CSM. The total machining energy was reduced by 13.28%. The total machining time was also reduced from 372.5 seconds to 325.17 seconds. In this approach, the time for VAAs/VATs was not altered but the total time was reduced. Therefore, the share of VAAs and VTTs increased and time efficiency was improved. It is also evident that the share of energy consumed by the 'coolant supply' Therblig was highest. The coolant pump used in the machine tool under consideration has the capacity of 1.1 kW. High rating and long running time of coolant pump lead to high energy consumption. Production and disposal of coolant result in high carbon emissions. This motivates the use of alternative cooling conditions such as minimum quantity lubrication

(MQL), mist cooling, etc. Also, the possibility to use a low capacity motor should be explored at the design stage.

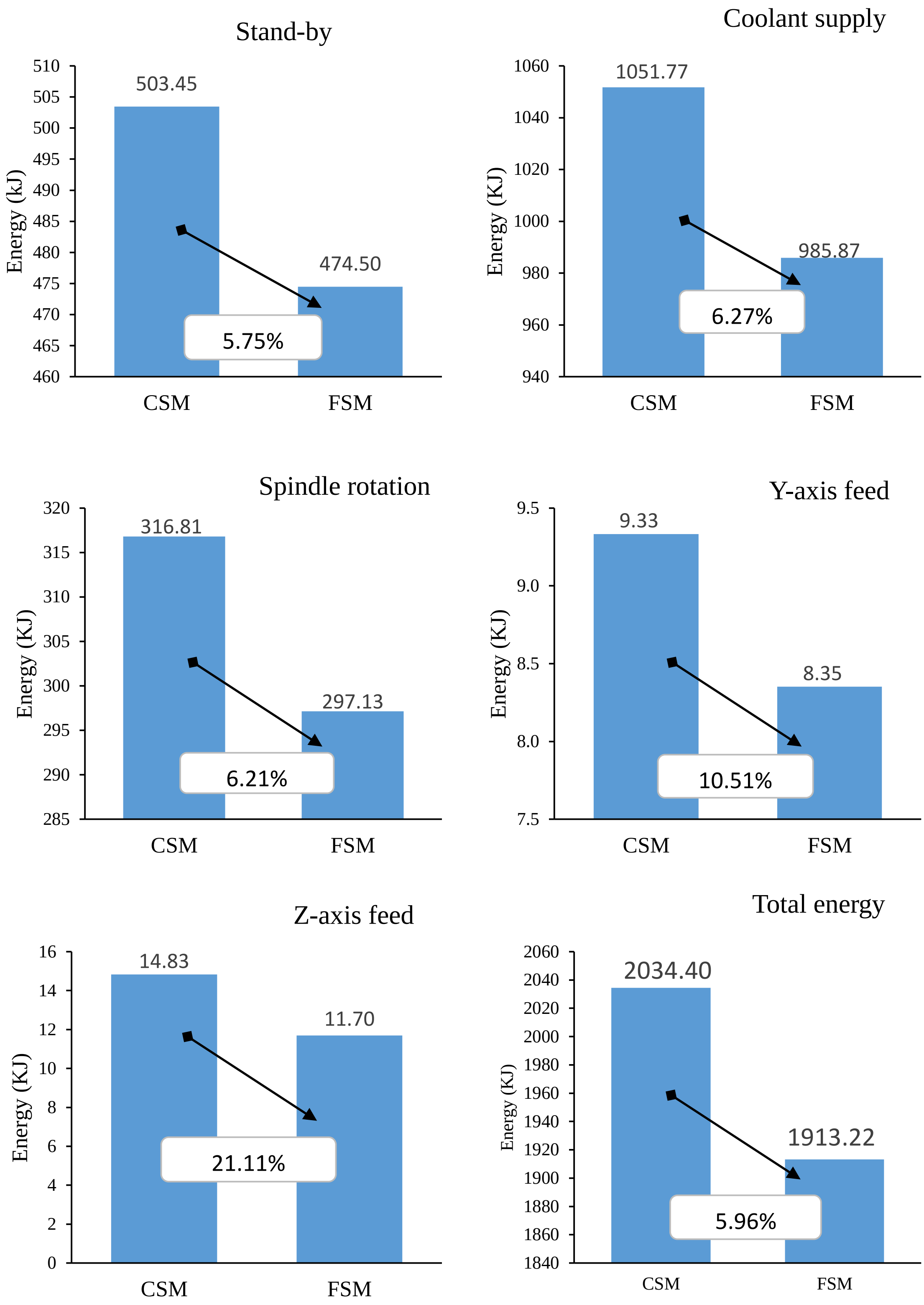

Figure 5.6 Energy demand reduction using the proposed methodology

The power for the stand-by condition was not high but the long duration of stand-by execution resulted into high-energy consumption. Power consumption by the y-axis and z-axis motors was reduced by 10.51% and 21.11%, respectively. It is observed that both, the cutting tool and machine table were moved to the home position for tool change in the CSM. However, only the tool was required to return to the home position for a tool change. Therefore, the NC code was modified to eliminate the rapid movement of the machine table for returning to home position while changing the tool. This reduced, both the processing time and energy consumption of the machining process in the FSM. Similarly, other time and energy wastes were identified and improved.

It is evident that the time efficiency (η_{time}), energy efficiency at activity level (η_A) and energy efficiency at Therblig level (η_T) were improved by 14.55%, 15.31%, and 15.41%, respectively as shown in Figure 5.7.

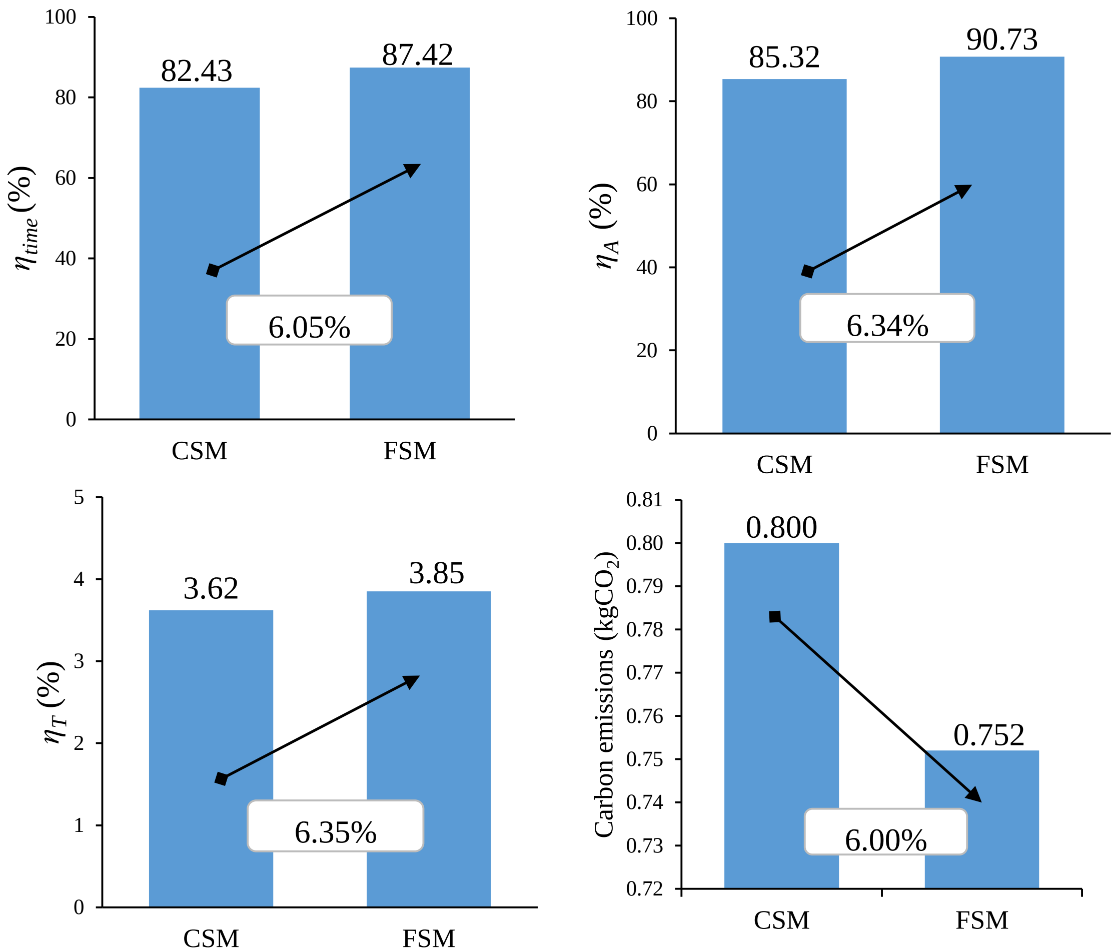

Figure 5.7 Comparison of time efficiency, energy efficiency and carbon emissions in CSM and FSM

The carbon emissions were reduced by 13.29%. It can also be noted that the value added time and cutting parameters were not altered in this study, so there was no effect on the quality. The energy consumption in transient states such as spindle acceleration or change of one state to another were not modelled in the study. Therefore, the energy predicted in the study was slightly lower than the measured energy as stated in section 5.3.3. The future work should consider the energy consumption by the transient states to improve the energy prediction accuracy.

5.5 CONCLUSIONS AND FUTURE RESEARCH DIRECTIONS

This chapter provided a micro analysis of milling process using value stream mapping method in conjunction with Therbligs. The methodology was used to identify the non-value added activities at the micro level. A milling case study was presented to validate the methodology. The case study showed an improvement of time efficiency (η_{time}), energy efficiency at activity level (η_A) and energy efficiency at Therblig level (η_T) by 6.05%, 6.34%, and 6.35%, respectively. The carbon emissions were reduced by 6.00%. This study did not alter the machining parameters or the value added time. Therefore, the product quality and tool life were not compromised.

The proposed methodology can also be used to develop energy stream maps for more than one machines in parallel to obtain the energy flow with respect to time and identify the peak load at the factory level. It can assist decision making for scheduling the various machining operations to reduce the peak load at factory level and development of potential energy and carbon emission reduction strategies during product design and process planning stages without compromising the product quality. This work can be further extended to other machining processes and coolant conditions such as minimum quantity lubrication or mist cooling. Future studies can focus on the effect of the tool path and feature processing sequence on energy consumption at the micro level. This study was conducted at the machine tool level. In future, the study can be extended to the production line level. The future work should consider the energy consumption by the transient states to improve the energy prediction accuracy. The technological aspects for improving the energy efficiency and carbon emissions of the machining processes should also be studied.